Photoaffinity Labeling of Diphtheria Toxin Fragment A with 8-Azidoadenosyl Nicotinamide Adenine Dinucleotide†

Rita Lodaya,‡ Steven R. Blanke,§,|| R. John Collier,§ and James T. Slama*,‡

Department of Medicinal and Biological Chemistry, College of Pharmacy, University of Toledo, Toledo, Ohio 43606, and Department of Microbiology and Molecular Genetics, Harvard Medical School, 200 Longwood Avenue, Boston, Massachusetts 02115

Received July 2, 1999; Revised Manuscript Received August 26, 1999

ABSTRACT: Diphtheria toxin fragment A (DT-A) is an important enzyme in the class of mono(ADP-ribosyl)transferases. To identify peptides and amino acid residues which form the NAD^+ binding site of DT-A using a photoaffinity approach, the photoprobes nicotinamide 8-azidoadenine dinucleotide (8-N_3-NAD) and nicotinamide 2-azidoadenine dinucleotide (2-N_3-NAD) were synthesized. Binding studies gave an IC_{50} of 2.5 μM for 8-N_3-NAD and 5.0 μM for 2-N_3-NAD. Irradiation of DT-A and low concentrations of [α-^{32}P]-8-N_3-NAD with short-wavelength UV light resulted in rapid covalent incorporation of the photoprobe into the protein. The photoincorporation was shown to be specific for the active site with a stoichiometry of photoincorporation of 75−80%. After proteolytic digestion of photolabeled DT-A, derivatized peptides were isolated using immobilized boronate affinity chromatography followed by reversed phase HPLC. Radiolabeled peptides originating from two regions of the protein were identified. Chymotryptic digestion produced labeled peptides corresponding to His^{21}−Gln^{32} and Lys^{33}−Phe^{53}. Lys-C digestion gave overlapping peptides Ser^{11}−Lys^{33} and Ser^{40}−Lys^{59}. Tyr^{27} was identified as the site of photoinsertion within the peptide His^{21}−Gln^{32} on the basis of the absence of PTH-Tyr at the predicted cycle during sequence analysis and by the lack of predicted chymotryptic cleavage at Tyr^{27}. Within the second modified peptide Ser^{40}−Lys^{59}, Trp^{50} is the most probable site of modification. Identification of Tyr^{27} as a site of photoinsertion is in agreement with its placement in the NAD binding site of the X-ray structure of the proenzyme DT−NAD complex [Bell, C. E., and Eisenberg, D. (1996) *Biochemistry 35*, 1137]. Trp^{50} is far from the adenine ring in the crystallographic model; however, site-directed mutagenesis studies suggest that Trp^{50} is a major determinant of NAD binding affinity [Wilson, B. A., Blanke, S. R., Reich, K. A., and Collier, R. J. (1994) *J. Biol. Chem. 269*, 23296−23301].

Diphtheria toxin is a 535-amino acid residue cytotoxic protein which is secreted from lysogenic strains of the pathogenic bacterium *Corynebacterium diphtheriae* (*1*−*3*). Proteolytic cleavage at a trypsin sensitive site (Arg^{190}, Arg^{192}, or Arg^{193}) and concomitant reduction of intrachain disulfide bonds produce two fragments. The N-terminal 190 amino acid residues constitute the enzymatically active A fragment (DT-A),[1] while the carboxy-terminal 345 amino acids constitute the B fragment (DT-B). DT-A catalyzes the transfer of the ADP-ribosyl moiety of NAD^+ to the modified histidyl residue (diphthamide) on elongation factor 2, thereby inhibiting protein synthesis in intoxicated cells. The B fragment is entirely responsible for binding the holotoxin to the surface of sensitive cells and its subsequent translocation into the cytoplasm.

The structure and enzymatic mechanism of DT-A is of interest because it is a paradigm for ADP-ribosyl transfer mechanisms, both within the family of microbial exotoxins and for the larger family of enzymes which includes constitutive mammalian ADP-ribosyl transferases. The primary structures of diphtheria toxin and its A fragment have been determined by chemical sequencing methods (*4*−*7*) and through determination of the cDNA sequence (*8*, *9*). The X-ray crystal structures of the DT dimer at 2.0 Å resolution and that of the DT monomer at 2.3 Å resolution have been determined (*10*, *11*). The structure of the isolated catalytic domain (equivalent to DT-A) was also determined at 2.5 Å resolution (*12*). In all cases, structures were elucidated with the endogenous inhibitor adenylyl (3′−5′) uridine 3′-monophosphate (ApUp) bound to the protein. More recently, the three-dimensional structure of dimeric DT bound to the substrate NAD was determined at 2.3 Å resolution (*13*), and

† This work was supported by grants from the NIH and from the deArce Foundation for Biomedical Research.

* To whom correspondence should be addressed: Department of Medicinal and Biological Chemistry, College of Pharmacy, University of Toledo, 2801 W. Bancroft St., Toledo, OH 43606-3390. Telephone: (419) 530-1925. Fax: (419) 530-7946. E-mail: jslama@uoft02.utoledo.edu.

‡ University of Toledo.

§ Harvard Medical School.

|| Current address: Department of Biology and Biochemistry, University of Houston, Houston, TX 77204.

[1] Abbreviations: EF-2, elongation factor 2; DICD, diisopropylcarbodiimide; DT, diphtheria toxin; DT-A, isolated catalytic domain of DT, consisting of residues 1−190; DTT, dithiothreitol; MALDI, matrix-assisted laser desorption ionization process for sample ionization in mass spectrometry; MES, 2-(*N*-morpholino)ethanesulfonic acid buffer ($pK_a = 6.15$); NMN, nicotinamide mononucleotide; PARP, poly(ADP-ribose) polymerase; PBA, phenylboronic acid; SDS−PAGE, sodium dodecyl sulfate−polyacrylamide gel electrophoresis; TCA, trichloroacetic acid.

10.1021/bi991528n CCC: $18.00
Published on Web 09/30/1999

the crystal structure of nucleotide-free dimeric DT was also determined at 2.3 Å resolution (*14*). However, a crystallographic model directly based on the analysis of the DT-A bound to NAD is not yet available.

Although these structural studies have yielded important information, the details of NAD binding to enzymatically active DT-A remain in doubt. We have used a photoaffinity approach to determine which peptides and amino acid residues interact with the bound ligand in solution. A photoaffinity approach using labeling with NAD^+ has already been successfully applied to DT-A (*15*, *16*) where catalytically essential Glu^{148} was specifically photoderivatized. In a latter study, 8-azidoadenine and 8-azidoadenosine photolabeled Tyr^{65} (*17*). In this paper, we report the results of a study using the substrate analogue 8-N_3-NAD to photolabel the purine binding domain of catalytically active DT-A. Isolation of photolabeled peptides by boronate affinity chromatography and reversed phase HPLC led to the identification of two sites of modification near the N-terminus of DT-A.

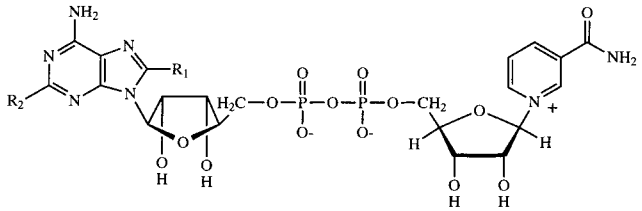

NAD^+:	$R_1 = H$	$R_2 = H$
8-N_3-NAD (**1**):	$R_1 = N_3$	$R_2 = H$
2-N_3-NAD (**2**):	$R_1 = H$	$R_2 = N_3$

EXPERIMENTAL PROCEDURES

Materials. Reagent grade organic and inorganic chemicals were purchased from Aldrich Chemical Co. (Milwaukee, WI) or Sigma (St. Louis, MO) and were used without further purification except as noted. Partially purified diphtheria toxin was obtained from Connaught Laboratories (Pasteur Mériux-Connaught, Swiftwater, PA). [^{14}C-*adenosyl*]NAD^+ was purchased from NEN Research Products (Boston, MA). Sequencing grade proteases (Arg-C and Lys-C) were from Boehringer-Manheim (Indianapolis, IN). Ecolite and Cytoscint for liquid scintillation counting were obtained from ICN (Costa Mesa, CA). Trifluoroacetic acid was from Applied Biosystems (Foster City, CA). PBA-30 resin, an affinity absorbant consisting of phenylboronic acid groups immobilized by attachment to agarose, was purchased from Amicon (Beverly Hills, MA). Tris-tricine ready gels and molecular mass standards were obtained from Bio-Rad (Richmond, CA). Biomax MR films (13 cm × 18 cm, Kodak) were used for autoradiography.

Isolation and Purification of DT-A. Partially purified diphtheria toxin was purified according to the procedure described by Carroll et al. (*18*). Briefly, the procedure included ion exchange chromatography on DEAE-Sephacel and conversion of the toxin into a completely "nicked" form by treatment with trypsin. The catalytic fragment A (DT-A) was finally obtained by treating a solution of nicked monomeric DT with dithiothreitol and urea and separating the A and B fragments by size-exclusion chromatography on Sephacryl S-200.

Isolation of EF-2 from Wheat Germ. Crude elongation factor 2 (EF-2) was obtained according to the procedure described by Carroll and Collier (*19*). Raw untoasted wheat germ was homogenized in a Waring blender. Cellular debris from the homogenate was removed by successive centrifugations at 21000*g* and 250000*g*. The postmicrosomal supernatant was fractionated with ammonium sulfate. Material precipitating between 30 and 50% saturation contained most of the EF-2 present in the postmicrosomal supernatant. The precipitate was dissolved and exhaustively dialyzed against the storage buffer.

NAD−EF-2 ADP-Ribosyl Transferase Assay. The initial rate of ADP-ribosyl transfer from NAD to EF-2 catalyzed by DT-A was determined by measuring the extent of incorporation of radioactivity from [^{14}C-*adenosyl*]NAD^+ (uniformly labeled in the adenine moiety) into trichloroacetic acid-precipitable material using partially purified EF-2 (*20*). The standard assay was conducted for 10 min at 25 °C and contained 50 mM Tris-HCl (pH 8.2), 1 mM EDTA, 10 mM β-mercaptoethanol, [^{14}C-*adenosyl*]NAD (0.85 μM), and DT-A (1.8 pmol) in a total volume of 100 μL.

Liquid Scintillation Counting. Radioactive samples were counted on a TM Analytic β-counter using appropriate windows for ^{14}C in the enzyme assay or ^{32}P for photolabeling experiments. Quench corrections were used when samples containing ^{14}C were counted. Liquid samples were counted with Ecolite (ICN). Cytoscint was used for assessing filters.

Reduction and Carboxymethylation of DT-A. DT-A was reduced in the presence of DTT and carboxymethylated with iodoacetate using the procedure of Chung and Collier (*21*).

Synthesis of Photoprobes. 8-N_3-NAD was synthesized as described by Koberstein (*22*) from nicotinamide mononucleotide (NMN) and 8-N_3-5′-AMP with modification. 8-N_3-5′-AMP was obtained and purified as described by Czarnecki et al. (*23*). For coupling 8-N_3-AMP with NMN to form the photoactive dinucleotide **1**, we found that a simple procedure utilizing carbodiimide-mediated coupling in aqueous solution (*24*) was convenient. β-NMN was soluble in the pyridine/water solvent system used for carbodiimide-mediated coupling and did not therefore require derivatization. 8-N_3-5′-AMP and a 4-fold excess of β-NMN were dissolved in a mixture of water and pyridine (1:5), and a 10-fold excess of 1,3-diisopropylcarbodiimide (DICD) was added. The mixture was stirred at 4 °C for 4 days with intermittent addition of small portions of DICD. The yields for the carbodiimide-mediated coupling ranged between 20 and 30%, but in our hands were comparable to those obtained through activation of the 8-N_3-5′-AMP as the P^1-nucleoside-5′-P^2-diphenylpyrophosphate (*25*). 2-N_3-NAD was synthesized according to the method described by Kim and Haley (*26*). Analysis of total phosphate for determining the concentrations of dinucleotides was conducted following the procedure of Ames (*27*).

[α-^{32}P]-8-N_3-NAD. [α-^{32}P]-8-N_3-5′-AMP was prepared enzymatically from 3′-AMP and coupled to β-NMN according to the procedure of Lodaya and Slama (*28*).

Photoaffinity Labeling. DT-A (5.0 μg, 230 pmol) was incubated with photoprobe (40 μM) in 20 mM MES (pH 6.0) in a final volume of 50 μL at 4 °C. Photolysis was performed with a hand-held short-wavelength (254 nm) UV lamp (2000 μW/cm^2, model UVG-54, UVP Inc., San Gabriel, CA) held at a fixed distance of 5 cm. Samples were irradiated

for 2.5 min. Duplicate 20 μL aliquots were precipitated by application onto TCA-impregnated paper, marked with a pencil in a series of numbered 1 in. × 1 in. squares. TCA paper was prepared using Whatman 3MM filter paper according to the procedure described by Carroll and Collier (*15*, *16*). The unbound photoprobe was removed by washing the filter paper with 5% aqueous TCA (2 × 15 min) followed by a 5 min wash with cold methanol. The filter paper was allowed to air-dry and was cut into squares. Radioactivity was determined by liquid scintillation counting (10 mL of Cytoscint). This analytical scale procedure was used to optimize reaction conditions, to determine specificity, and to measure the stoichiometry of the photolabeling reaction.

Preparative Photolabeling and Enzymatic Digestion of DT-A. DT-A (200−400 μg) was photolabeled with [α-^{32}P]-8-N_3-NAD (protein:probe molar ratio of 1:5, specific activity of 0.17−0.65 mCi/mmol) for 2.5 min at 4 °C in 20 mM MES buffer (pH 6.5). The protein concentration was 1 mg/mL. The photolabeled protein was precipitated by adding 20% v/v ice-cold TCA (final concentration of ca. 6%). After incubation on ice for 30 min, the pellet was recovered by centrifugation and was washed two times with ice-cold methanol.

(i) Trypsin Digestion. Pelleted photolabeled DT-A was resuspended in 100 mM ammonium acetate (pH 8.0); trypsin (2 μg/100 μg of DT-A) was added (from a 1 mg/mL stock in 1 mM HCl), and the mixture was incubated at 34 °C for 24 h followed by another addition of trypsin (10 μg/100 μg of DT-A) and incubation at 37 °C for 24 h. Analysis by SDS−PAGE indicated that the photoderivatized protein remained undigested under the conditions described above.

(ii) Chymotrypsin Digestion. Photolabeled DT-A was resuspended in 100 mM ammonium acetate (pH 8.0) containing 10 mM $CaCl_2$ and 2 M urea and digested with chymotrypsin (4 μg/100 μg of DT-A) at 25 °C for 20 h.

(iii) Lys-C Digestion. Photolabeled DT-A was resuspended in 100 mM ammonium acetate (pH 8.0) containing 1 mM EDTA and 2 M urea and digested with Lys-C (3 μg/100 μg of DT-A) at 37 °C for 24 h.

(iv) Arg-C Digestion. Photolabeled DT-A was resuspended in 100 mM ammonium acetate (pH 8.0) containing 10 mM $CaCl_2$, 10 mM DTT, 1 mM EDTA, and 2 M urea and digested with Arg-C (2 μg/100 μg of DT-A) at 37 °C for 20 h.

SDS−PAGE. Digestions were monitored by SDS−PAGE using 16.5% Tris-tricine ready gels (Bio-Rad) with a 4% stacking gel according to the method of Schägger and von Jagow (*29*). Gels were run at a constant voltage of 100 mV. Gels were stained with Coomassie blue G-250 solution (0.025%) for 1 h, after immersing in a fixative solution for 30 min. Gels were destained in a 10% acetic acid solution overnight. After soaking in a solution containing 3−5% glycerol in 10% acetic acid and 20% methanol for 3 h, gels were dried at 60 °C for 4 h on a slab gel dryer and subjected to autoradiography.

Immobilized Boronate Affinity Chromatography. The digested protein was diluted with 100 mM ammonium acetate (pH 8.9) (buffer A, 1.5 mL) and applied onto 4.0 mL of PBA-30 (Amicon) preequilibrated with buffer A. The resin was washed successively with 20 mL of buffer A, 20 mL of buffer A containing 0.5 M NaCl, 20 mL of buffer A, 20 mL of buffer A containing 4 M urea, and 20 mL of buffer A. The photolabeled peptides were eluted with 50 mM ammonium acetate containing 50 mM sorbitol (pH 8.9) followed by the same buffer containing 100 mM sorbitol. Fractions (1.0 mL) were collected during chromatography, and radioactivity was determined by liquid scintillation counting.

Reversed Phase HPLC. Radioactive peaks obtained from immobilized boronate affinity chromatography were further purified by reversed phase HPLC on a Vydac C4 column (150 mm × 4.6 mm, 10 μm, 300 Å). The conditions that were used were 2% solvent B at 0 min, 2% solvent B at 10 min, 35% solvent B at 70 min, 75% solvent B at 90 min changed linearly, and 98% solvent B at 105 min (solvent A being 0.06% trifluoroacetic acid in water and solvent B being 0.052% trifluoroacetic acid in 70% acetonitrile/30% H_2O). The flow rate was 0.5 mL/min, and 1 mL fractions were collected. The UV absorbance (215 nm) was monitored by an SM 4000 programmable wavelength detector (LDC analytical). Fractions containing radioactivity were pooled, concentrated on a centrifugal concentrator, and subjected to amino acid sequence analysis.

Sequence Analysis. Automated Edman degradation was performed on Applied Biosystems gas or pulsed liquid phase model 470A and 477A sequenators equipped with a phenylthiohydantoin amino acid analyzer (model 610A) at the University of Michigan Protein and Carbohydrate Structure Facility (Ann Arbor, MI). Typically, several peaks were obtained in a cycle that coeluted with standard PTH-amino acid markers. The amino acid in any given cycle was assigned by the Structure Facility on the basis of the picomolar yield of a PTH-amino acid derivative and its increase in quantity over that in the previous cycle. The data reported for sequencing results are those of the yield in picomoles of the assigned PTH-amino acid derivative in the reported cycle.

RESULTS

Binding of Photoprobes to DT-A. 8-N_3-NAD (**1**) and 2-N_3-NAD (**2**) were tested for their ability to inhibit the enzymatic activity of DT-A. The ADP-ribosyl transferase activity of DT-A was assayed in the presence of increasing concentrations of the analogues mentioned above. The initial rate of ADP-ribosyl transfer from NAD to EF-2 catalyzed by DT-A was determined by measuring the incorporation of radioactivity from [^{14}C-*adenosyl*]NAD^+ into trichloroacetic acid-precipitable material using partially purified EF-2. IC_{50} values for 8-N_3-NAD **1** and 2-N_3-NAD **2** were determined to be 2.3 and 4.8 μM, respectively (Figure 1). The dissociation constant for NAD determined for DT-A is about 8−10 μM (*30*). Hence, both the modified nucleotides **2** and **3** interact strongly with DT-A and could potentially be used as photoaffinity labels. The ability of 8-N_3-NAD to act as a substrate for the ADP-ribosyl transferase reaction was assessed by measuring trichloroacetic acid-precipitable radioactivity upon incubation of increasing concentrations of [α-^{32}P]-8-N_3-NAD in the presence of DT-A and EF-2. Results confirm that 8-N_3-NAD was a substrate for DT-A (data not shown).

Photoaffinity Labeling. Irradiation of 4.6 μM DT-A and 15 μM [α-^{32}P]-8-N_3-NAD for 2.5 min with short-wavelength UV light led to the covalent labeling of the protein (Figure 2). This was observed qualitatively when the photoderivatized

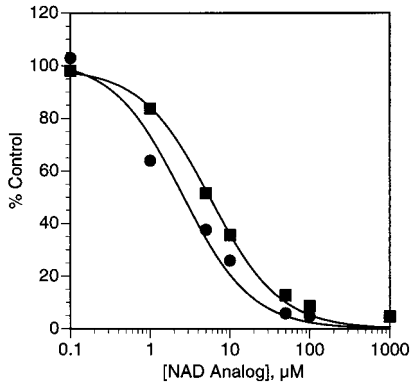

FIGURE 1: Inhibition of the ADP-ribosyl transferase activity of DT-A by 8-N_3-NAD and 2-N_3-NAD. Varying amounts of 8-N_3-NAD (●) or 2-N_3-NAD (■) were added to an assay containing DT-A (1.8 pmol), [^{14}C-*adenosyl*]NAD (0.85 μmol), and partially purified EF-2, and the enzymatic assay was conducted as described in Experimental Procedures.

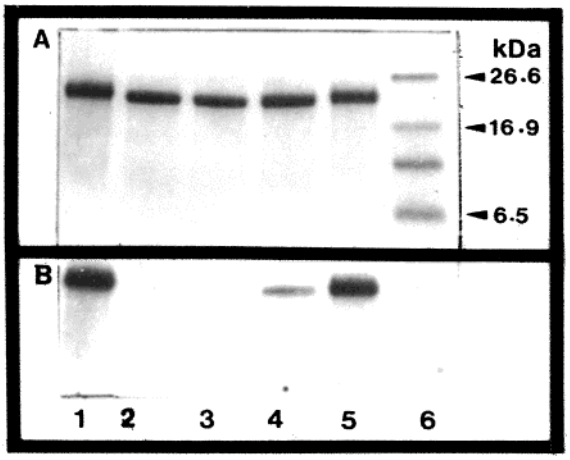

FIGURE 2: SDS−PAGE of photoaffinity labeling of DT-A with [α-^{32}P]-8-N_3-NAD. DT-A (2.5 μg) was incubated with the photoprobe (30 μM) in 20 mM MES buffer (pH 6). Panel A shows the Comassie blue-stained gel, while panel B shows the autoradiogram. Lanes are identified as follows: lanes 1 and 5, DT-A and photoprobe irradiated for 2.5 min; lane 2, DT-A and photoprobe incubated together for 2.5 min in the dark; lane 3, photoprobe irradiated for 2.5 min followed by immediate addition of DT-A and incubation for 2.5 min in the dark; and lane 4, photoprobe irradiated for 2.5 min followed by immediate addition of DT-A and irradiation for an additional 2.5 min.

protein was analyzed by SDS gel electrophoresis followed by autoradiography, where a heavily labeled 22 kDa band isographic with DT-A was observed. No labeling was detected when the protein and [α-^{32}P]**1** were incubated together in the dark, or if [α-^{32}P]**1** was irradiated prior to the addition of protein. When photoderivatization was conducted in the presence of 50 or 100 μM NAD^+, the amount of photoincorporated label decreased significantly as shown by the lighter bands on the autoradiogram (Figure 3). Addition of 100 μM ATP or AMP resulted in only small changes to the band's intensity, while 100 μM adenine, a potent competitive inhibitor of dinucleotide binding, decreased band intensities moderately.

Quantitative photoaffinity labeling experiments were performed to optimize conditions for the photoinsertion, to verify the specificity of the reaction for the active site, and to determine the stoichiometry of the reaction. After irradiation of DT-A in the presence of low concentrations of

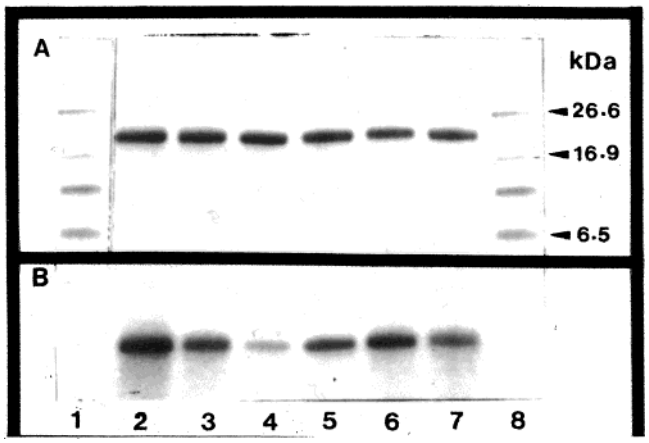

FIGURE 3: Effect of the added NAD^+ or nucleotides on the photoderivatization of DT-A with [α-^{32}P]-8-N_3-NAD. (A) Comassie blue-stained gel and (B) autoradiogram. Photoderivatization of DT-A was conducted as described in the legend of Figure 2. Lanes 1 and 8 contained molecular mass markers. Lanes 2−7 show the results of photoderivatization of DT-A with [α-^{32}P]-8-N_3-NAD (15 μM) either alone (lane 2) or in the presence of 50 μM NAD^+ (lane 3), 100 μM NAD^+ (lane 4), 100 μM ATP (lane 5), 100 μM AMP (lane 6), or 100 μM adenine (lane 7).

photoprobe under various conditions, the amount of photoprobe covalently bound to protein was determined by measuring the amount of protein−nucleotide conjugate as acid-precipitable radioactivity. The photoinsertion reaction reached its maximum value after irradiation for 2.5 min at 4 °C. Over the pH range of 5.3−9.2, the efficiency of photoinsertion reached a maximum at pH 6.0, a value 2-fold higher than that obtained at pH 8.2, the pH optimum for the enzymatic ADP-ribosyl transfer reaction. The presence of divalent ions such as Zn^{2+}, Ca^{2+}, and Mg^{2+} or the presence of EDTA did not significantly affect the photoinsertion reaction, although the photoinsertion was found to be more efficient in low-ionic strength solutions. The stoichiometry of labeling under optimal conditions of photoinsertion (20 mM MES buffer at pH 6 and 4 °C with 15 μM **1**) as determined by acid-precipitable radioactivity was approximately 85%.

Experiments were performed to establish the specificity of the photoderivatization reaction. Irradiation was required for photoinsertion (Figure 4). Pre-photolysis of the photoprobe prior to addition of the enzyme prevented covalent insertion of the dinucleotide. Pre-photolysis of the photoprobe followed by addition of the enzyme and subsequent irradiation resulted in a photoinsertion level which was less than 3% of the control. The ability of NAD, ATP, AMP, adenosine, and adenine to inhibit photoinsertion of 8-N_3-NAD was also quantitatively determined. In this experiment, addition of 100 μM NAD or 100 μM adenine to the reaction mixture afforded 87 and 70% photoprotection, respectively, whereas identical concentrations of ATP, AMP, and adenosine afforded less than 10% photoprotection. These observations are consistent with the binding affinity of these compounds for DT-A as determined by Kandel et al. (*30*).

The effect of varying the initial concentration of the photoprobe on the amount of nucleotide covalently inserted in the protein is shown in Figure 5A. When 5 μg of 4.6 μM DT-A was photolabeled with increasing concentrations of radiolabeled **1** (0−100 μM), the extent of photolabeling increased but reached a maximum value at about 60 μM **1**.

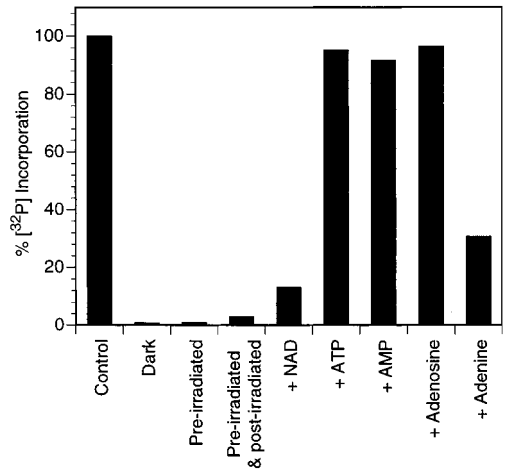

FIGURE 4: Determination of the amount of covalent photoinsertion into DT-A under varying conditions. DT-A (5.0 μg) was incubated for 5 min in 50 mL of 20 mM MES buffer (pH 6.0) containing [α-^{32}P]-8-N_3-NAD (15 μM). For the column labeled Control, this solution was irradiated for 2.5 min. For the column labeled Dark, the solution was incubated in the dark for 2.5 min. For the column labeled Pre-irradiated, the solution was irradiated for 2.5 min in the absence of enzyme, the enzyme added, and the mixture incubated for 2.5 min in the dark. For the lane labeled Pre-irradiated & post-irradiated, the solution was irradiated for 2.5 min in the absence of the enzyme, the enzyme added, and the mixture irradiated again for 2.5 min. To determine the effect of the presence of low concentrations of various compounds on photoinsertion, the solution of DT-A was incubated with the designated compound at a concentration of 100 μM for 5.0 min, [α-^{32}P]-8-N_3-NAD added, and the solution irradiated for 2.5 min at 4 °C. At the conclusion of each experiment, a 20 μL aliquot was removed and added to TCA-saturated paper and the amount of nucleotide covalently bound to the protein determined by liquid scintillation counting as described in Experimental Procedures.

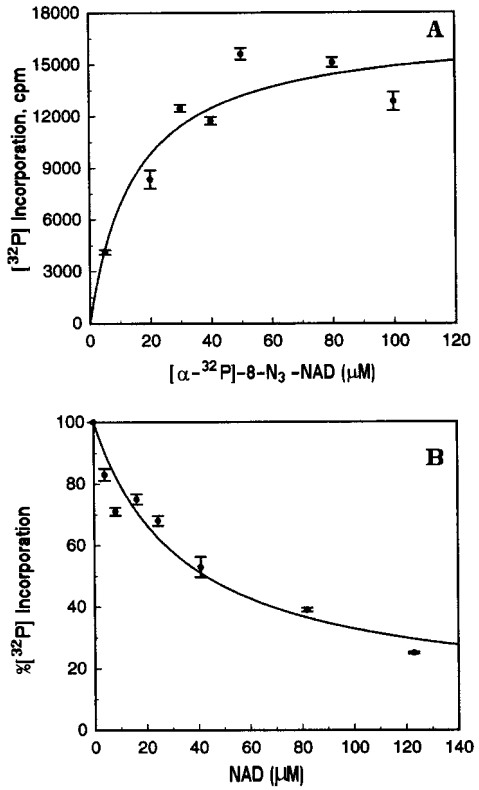

FIGURE 5: Effect of varying the concentration of [α-^{32}P]-8-N_3-NAD on its photoincorporation into DT-A (A) or protection of DT-A from photoderivatization by [α-^{32}P]-8-N_3-NAD by varying concentrations of NAD^+ (B). (A) DT-A (5 μg) in 50 μL of MES buffer (pH 6) was incubated with [α-^{32}P]-8-N_3-NAD (0−100 μM) at 0 °C and irradiated with short-wavelength UV light for 2.5 min. The level of covalent incorporation of [^{32}P]**1** was determined as acid-precipitable radioactivity as described in the legend of Figure 4 and in Experimental Procedures. Data were fit to the equation $cpm = cpm_\infty[\mathbf{1}]/(K_d + [\mathbf{1}])$ using nonlinear regression analysis, and the values for cpm_∞ and K_d were calculated. The solid line represents the theoretical line calculated using the empirically determined values of cpm_∞ and K_d (17 116 cpm and 15 μM, respectively). (B) DT-A was treated with NAD^+ (0−100 μM) and 15 μM [^{32}P]**1**, and the extent of photolabeling into protein was determined as described above. Data were fit to the equation $\%\ \text{incorporation} = 100\% - \%_\infty[\mathbf{1}]/(K_d + [\mathbf{1}])$ using nonlinear regression analysis, and the values for $\%_\infty$ and K_d were calculated. The solid line represents the theoretical line calculated using the empirically determined values of $\%_\infty$ and K_d (90% and 34 μM, respectively).

Saturation of photoinsertion occurred with an apparent K_d for **1** of 15 ± 7 μM. When the protein was labeled under identical conditions except for NAD^+ being added, the level of covalent photolabeling was observed to decrease significantly (Figure 5B). About 120 μM NAD was able to reduce the level of photoinsertion by 15 μM [α-^{32}P]**1** by 75% with an apparent K_d for NAD^+ of 35 μM.

The primary sequence of DT-A contains a single cysteine at position 186 which is known to be excluded from the NAD binding site. Since SH groups can react nonspecifically with nitrenes, we determined the portion of our photoderivatization reaction that was due to reaction through Cys^{186}, by measuring the level of photoincorporation into reduced and carboxymethylated protein (RCM−DT-A). There was little difference between photoinsertion into DT-A and photoinsertion into RCM−DT-A (Table 1). Photoprotection in the presence of 100 μM NAD and 100 μM ATP suggested that no more than 5−10% of the photoincorporation could be due to reaction of the photoprobe with cysteine.

Isolation of Photolabeled Peptides. To identify the peptides which were modified by 8-N_3-NAD, DT-A (200−400 μg, 46 μM) was photolabeled under optimal conditions and the unbound photoprobe removed by precipitation of the protein with 6−10% trichloroacetic acid. The precipitated photoderivatized DT-A was washed, resuspended in buffer, and subjected to proteolysis. Photolabeled DT-A was found to be resistant to tryptic digestion. Chymotrypsin, endoproteinase Lys-C, and endoproteinase Arg-C were each used to digest the photoderivatized protein. SDS−PAGE and autoradiography of aliquots taken from digestion mixtures after 24 h showed the absence of the unproteolyzed photoderivatized protein band at 22 kDa and the presence of a thick

Table 1: Photoincorporation of [α-^{32}P]-8-N_3-NAD into RCM−DT-A[a]

conditions[b]	relative level of ^{32}P incorporation (%)
DT-A	100
DT-A and ATP[c]	95
DT-A and NAD	18
RCM−DT-A and ATP[c]	90
RCM−DT-A and NAD	8

[a] RCM−DT-A was obtained by reduction and carboxymethylation of DT-A according to the procedure of Chung and Collier (*21*). [b] Conditions for photolabeling and determination of the level of ^{32}P incorporation were as described in the legend of Figure 4. [c] ATP was added to correct for the inner filter effect and enable direct comparison with labeling in the presence of NAD.

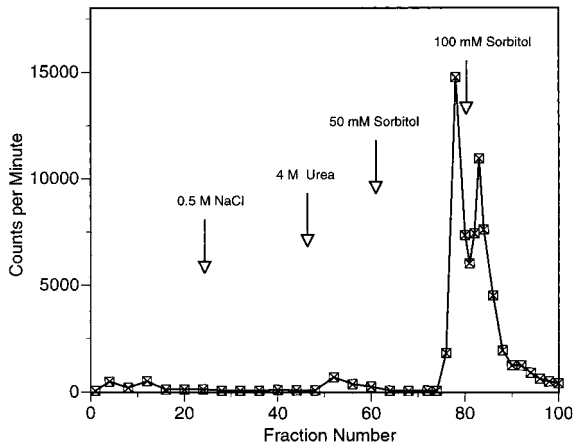

FIGURE 6: Immobilized boronate affinity chromatography of chymotrypsin-digested photoderivatized DT-A. DT-A (400 mg, 18.9 nmol) was photolabeled with 106 nmol of [α-^{32}P]-8-N_3-NAD and digested with chymotrypsin as described in Experimental Procedures. The digest was loaded onto an immobilized boronate column equilibrated with 0.1 M NH_4OAc (pH 8.9) (buffer A). The designated eluents were mixed with buffer A as indicated in the figure. The bound material specifically eluted into buffer A containing 0.05 M sorbitol. Fractions (1.5 mL) were collected, and radioactivity was determined by liquid scintillation counting.

band of labeled peptides migrating with apparent molecular masses between 6 and 8 kDa.

Chymotryptic Digestion. Photolabeled DT-A was proteolyzed by chymotrypsin as described in Experimental Procedures. The resulting peptide fragments containing covalently attached photoprobe were purified by immobilized boronate affinity chromatography (*31*, *32*) which takes advantage of the specific binding of the two *cis*-diols of the dinucleotide to columns containing immobilized *p*-aminophenylboronic acid. At high pH, peptides modified with [α-^{32}P]-8-N_3-NAD as well as any unbound photoprobe were selectively bound by the phenyl boronate agarose resin, whereas unmodified peptides eluted from the column in the void volume. The radioactivity profile of immobilized boronate affinity chromatography of a chymotryptic digest of DT-A photolabeled with [α-^{32}P]-8-N_3-NAD is shown in Figure 6. Peptides bound to this column due to nonspecific ionic or hydrophobic interactions were removed by washing with 0.5 M NaCl and 4 M urea. Photolabeled peptides were selectively eluted into a buffer containing 50−100 mM sorbitol, a polyalcohol that competes with dinucleotide for boronate binding at pH 8.9.

Radioactive fractions isolated via boronate affinity chromatography were further purified by chromatography on a C4 reversed phase HPLC column using a linear gradient formed between aqueous trifluoroacetic acid (TFA) and 70% acetonitrile containing TFA. The first six fractions collected after application of the sample to the boronate column were pooled for analysis and lyophilized as were the fractions which eluted into 100 mM NH_4OAc (pH 8.9). HPLC analysis indicated that the fractions collected immediately after the application of the sample contained a complex mixture of nonradioactive peptides and therefore suggests that peptides which did not contain covalently bound dinucleotide failed to bind to the boronate resin under the conditions of our chromatography. The fractions which bound to the column and which were eluted into buffer containing sorbitol were pooled and further purified by reversed phase HPLC. Profiles of radioactivity versus the fraction number of the reversed

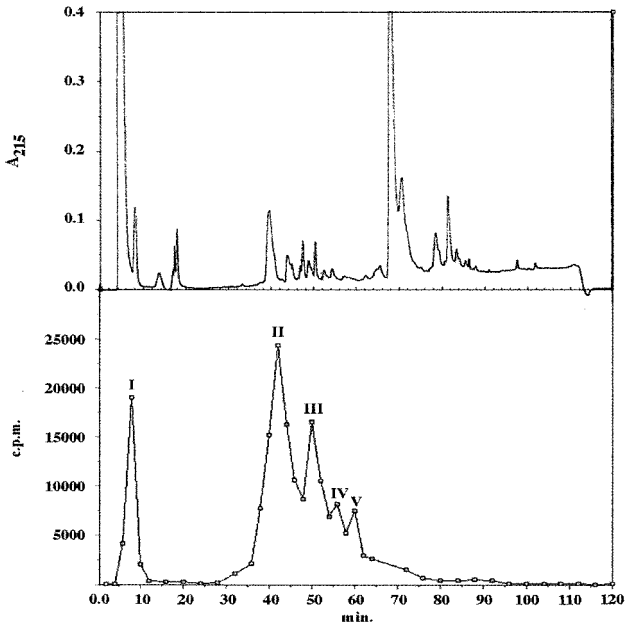

FIGURE 7: Reversed phase HPLC of radioactive fractions obtained from immobilized boronate affinity chromatography of a chymotryptic digest of photolabeled DT-A. The column (C4, 10 μm, 4.6 mm × 150 mm) was equilibrated in 98% buffer A (0.06% TFA) and 2% buffer B (0.052% TFA and 70% CH_3CN). The material from the pooled fractions (Figure 6) was injected into the system, and the column was eluted at a flow rate of 0.5 mL/min. The gradient formed between buffers A and B is described in Experimental Procedures. Fractions (1 mL) were collected, and the radioactivity of the aliquots was determined.

phase HPLC separation of pooled fractions that eluted from the boronate column with sorbitol exhibited five peaks (Figure 7): one (peak I) at the beginning of the gradient and coincident with the void volume and four peaks eluting between fractions 19 and 30 (peaks II−V in Figure 7). Peaks I−V were individually collected, concentrated under reduced pressure, and submitted to automated Edman degradation in an effort to determine the N-terminal sequence of the peptides.

Peaks I and III were determined to be nonpeptidyl by the failure to produce recognizable PTH derivatives. The radioactivity under peak I is most likely due to released photoinserted dinucleotide, since it appears at a position in the chromatogram where nonpeptidyl, irradiated [α-^{32}P]-8-N_3-NAD derivatives elute. The lability of photoinsertion products under HPLC conditions is known (*33*). Peak III could be a product of the irradiated photoprobe which has a higher affinity for the C4 column, an N-terminal blocked peptide, or a hydrophobic purine derivative. Peak II contained the major photoderivatized peptide beginning with an N-terminal His (Table 2). The determined sequence for this peptide corresponds well to a sequence close to the N-terminus of DT-A, His^{21}−Gln^{32}. Peaks IV and V contained peptides which produced a common N-terminal Lys and continuing through a carboxy-terminal Asp and Trp, respectively, corresponding closely to the DT-A sequence Lys^{33}−Trp^{50} (see Table 2). For peak II, PTH-Tyr was not detected at cycle 7 as predicted by the sequence of DT-A. Chymotrypsin additionally failed to cleave at this residue (Tyr^{27}), and the sequence continued ending at Gln^{32}.

Lys-C Digestion. In another set of experiments, DT-A was photolabeled with [α-^{32}P]-8-N_3-NAD under similar condi-

Table 2: N-Terminal Sequence Analysis of Photolabeled Chymotryptic Peptides after Boronate Affinity and HPLC Purification

chymotryptic peptide 1					chymotryptic peptide 2					
peak II					peak IV					peak V
	PTH-amino acid yield (pmol)			predicted		PTH-amino acid yield (pmol)			predicted	
cycle	expt 1	expt 2	expt 3	residue	cycle	expt 1[a]	expt 2[b]	expt 3	residue	expt 1
1	H (17)	H (8)	H (6)	His^{21}	1	K (52)	K (25)	K (6)	Lys^{33}	K (20)
2	G (259)	G (107)	G (100)	Gly^{22}	2	G (86)	G (47)	G (25)	Gly^{34}	G (42)
3	T (65)	T (31)	T (27)	Thr^{23}	3	I (22)	I (8)	I (6)	Ile^{35}	I (7)
4	K (77)	K (17)	K (20)	Lys^{24}	4	Q (26)	Q (8)	Q (7)	Gln^{36}	Q (8)
5	P (69)	P (20)	P (12)	Pro^{25}	5	K (28)	K (4)	K (3)	Lys^{37}	K (4)
6	G (100)	G (41)	G (25)	Gly^{26}	6	P (20)	P (6)	P (2)	Pro^{38}	P (4)
7	ND[c]	ND[c]	ND[c]	Tyr^{27}	7	K (17)		K (1)	Lys^{39}	K (3)
8	V (37)	V (11)	V (6)	Val^{28}	8	S (13)		S (1)	Ser^{40}	S (2)
9	D (50)	D (15)	D (8)	Asp^{29}	9	G (21)		G (7)	Gly^{41}	G (12)
10	S (15)	S (6)	S (3)	Ser^{30}	10	T (6)		T (1)	Thr^{42}	T (2)
11	I (5)	I (5)	I (3)	Ile^{31}	11			Q (2)	Gln^{43}	Q (3)
12	Q (14)	Q (4)	Q (2)	Gln^{32}	12			G (7)	Gly^{44}	G (11)
					13			N (2)	Asn^{45}	N (3)
					14			Y (1)	Tyr^{46}	Y (1)
					15			D (2)	Asp^{47}	D (3)
					16			D (2)	Asp^{48}	D (3)
					17			D (2)	Asp^{49}	D (4)
					18			W (0.4)	Trp^{50}	

[a] Sequencing was terminated after ten cycles. [b] Sequencing was terminated after six cycles. [c] ND indicates that no identifiable amino acid derivative could be detected.

tions and subjected to proteolysis with endoproteinase Lys-C. Photoderivatized peptides were separated from the underivatized peptides by boronate affinity chromatography and further purified by C4 reversed phase HPLC. Again, analysis of the nonradioactive fractions collected during sample application to the boronate affinity column by reversed phase HPLC showed a complex mixture of unlabeled peptides. The result of the boronate affinity chromatography was identical to that obtained from the chymotryptic digest and shown in Figure 6. The HPLC profile of the pooled fractions that specifically eluted from the boronate affinity column in buffer containing sorbitol is shown in Figure 8. Three major peaks (I−III) were observed. Upon sequence analysis, peak I was determined to be nonpeptidyl. Peak II revealed a sequence corresponding to $Ser^{40}-Lys^{59}$, whereas peak III corresponded to the sequence $Ser^{11}-Lys^{33}$ (Table 3). Thus, overlapping sequences were obtained from derivatized chymotryptic and Lys-C digests. Peak II in the Lys-C digest corresponds to the peptide which overlaps with peak IV in the chymotryptic digest ($Lys^{33}-Phe^{53}$). In the case of the Lys-C digest, this peptide begins at Ser^{40}. In peak II, PTH-Trp at cycle 11 was obtained in very low yields and cleavage by Lys-C was impeded at the next residue which is Lys^{51}. This peptide could be sequenced up to Tyr^{54}. Peptide $Ser^{11}-Lys^{33}$ (peak III) in the Lys-C digest overlaps with the major chymotryptic peptide $His^{21}-Gln^{32}$. Thus, the sequences of overlapping peptides obtained from chymotryptic and Lys-C digests indicate that the sites of photoinsertion must be within the common sequences $His^{21}-Gln^{32}$ and $Ser^{40}-Phe^{53}$.

Arg-C Digestion. Endoproteinase Arg-C was used as the third protease with which to obtain fragments of photolabeled DT-A. The Arg-C digest was subjected to immobilized boronate affinity chromatography as described previously. A chromatographic profile similar to the previous experiment using Lys-C digestion was obtained. Further purification on C4 reversed phase HPLC again gave a profile similar to that of the Lys-C digest, resulting in the isolation of three major

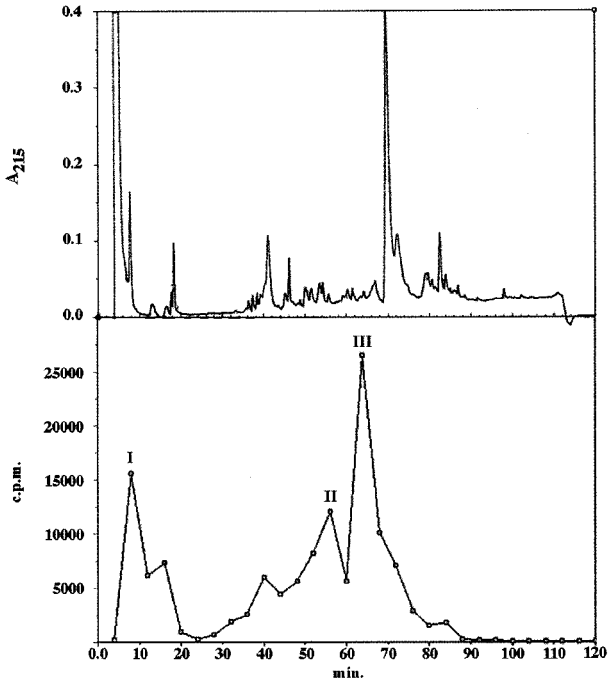

FIGURE 8: Purification of photoderivatized peptides from the Lys-C digest by reversed phase HPLC. The radioactive fractions were obtained from immobilized boronate affinity chromatography of a Lys-C digest of photolabeled DT-A. Pooled and concentrated fractions were loaded onto a C4 column, and chromatography was developed as described in the legend of Figure 7.

radioactive peaks (chromatography not shown). The first peak eluting at the void volume was nonpeptidyl. Sequence analyses of peaks II and III (Table 4) indicated that endoproteinase Arg-C unexpectedly cleaved the modified protein at lysyl residues. Instead of the predicted large N-terminal peptide ($Gly^{1}-Arg^{126}$) being obtained which would result from specific cleavage after Arg^{120}, peak II contained a peptide that began at Gly^{34} and was sequenced through Asp^{49}. Peak III contained a peptide which was identical to the Lys-C peptide $Ser^{11}-Pro^{25}$. The results of

Table 3: N-Terminal Sequence Analysis of Photolabeled Lys-C Peptides after Boronate Affinity and HPLC Purification

Lys-C peptide 1				Lys-C peptide 2			
peak III				peak II			
	PTH-amino acid yield (pmol)				PTH-amino acid yield (pmol)		
cycle	expt 1	expt 2	predicted residue	cycle	expt 1	expt 2	predicted residue
1	S (47)	S (26)	Ser[11]	1	S (86)	S (48)	Ser[40]
2	F (74)	F (17)	Phe[12]	2	G (135)	G (75)	Gly[41]
3	V (36)	V (19)	Val[13]	3	T (38)	T (28)	Thr[42]
4	M (33)	M (10)	Met[14]	4	Q (57)	Q (22)	Gln[43]
5	E (42)	E (11)	Glu[15]	5	G (106)	G (37)	Gly[44]
6	N (37)	N (24)	Asn[16]	6	N (47)	N (24)	Asn[45]
7	F (23)	F (9)	Phe[17]	7	Y (40)	Y (11)	Tyr[46]
8	S (7)	S (6)	Ser[18]	8	D (27)	D (9)	Asp[47]
9	S (9)	S (7)	Ser[19]	9	D (45)	D (11)	Asp[48]
10	Y (17)	Y (7)	Tyr[20]	10	D (36)	D (12)	Asp[49]
11	H (2)	H (2)	His[21]	11	W (2)	W (1)	Trp[50]
12	G (31)	G (10)	Gly[22]	12	K (3)	K (2)	Lys[51]
13	T (3)	T (5)	Thr[23]	13	G (11)	G (11)	Gly[52]
14	K (3)	K (2)	Lys[24]	14	F (4)	F (2)	Phe[53]
15	P (7)	P (2)	Pro[25]	15	Y (4)	Y (2)	Tyr[54]

Table 4: N-Terminal Sequence Analysis of Photolabeled Arg-C Peptides after Boronate Affinity and HPLC Purification

Arg-C peptide 1				Arg-C peptide 2			
peak III				peak II			
	PTH-amino acid yield (pmol)				PTH-amino acid yield (pmol)		
cycle	expt 1	expt 2	predicted residue	cycle	expt 1	expt 2[a]	predicted residue
1	S (32)	S (34)	Ser[11]	1	G (64)	G (160)	Gly[34]
2	F (10)	F (30)	Phe[12]	2	I (22)	I (32)	Ile[35]
3	V (10)	V (23)	Val[13]	3	Q (22)	Q (33)	Gln[36]
4	M (5)	M (17)	Met[14]	4	K (12)	K (26)	Lys[37]
5	E (6)	E (17)	Glu[15]	5	P (6)	P (28)	Pro[38]
6	N (10)	N (16)	Asn[16]	6	K (6)	K (19)	Lys[39]
7	F (6)	F (16)	Phe[17]	7	S (3)		Ser[40]
8	S (4)	S (7)	Ser[18]	8	G (14)		Gly[41]
9	S (3)	S (6)	Ser[19]	9	T (5)		Thr[42]
10	Y (3)	Y (9)	Tyr[20]	10	Q (1)		Gln[43]
11	H (1)	H (2)	His[21]	11	G (13)		Gly[44]
12	G (8)	G (20)	Gly[22]	12	N (3)		Asn[45]
13	T (2)	T (3)	Thr[23]	13	Y (1)		Tyr[46]
14	K (1)		Lys[24]	14	D (3)		Asp[47]
15	P (1)		Pro[25]	15	D (3)		Asp[48]
				16	D (4)		Asp[49]

[a] Sequencing was terminated after six cycles.

Arg-C proteolysis parallel those obtained by Lys-C digestion and confirm the identification of the photoderivatized peptides.

A summary of sequence analyses of the overlapping modified peptides obtained from DT-A photolabeled with 8-N_3-NAD is presented in Figure 9. Photoderivatized peptides isolated from reversed phase HPLC of all three digests described above were submitted for mass spectrometry at the Protein Structure Facility at Michigan State University. Analysis by MALDI (using α-hydroxycinnamic acid as well as sinapinic acid containing ionization matrix), fast atom bombardment, and electrospray ionization failed to produce molecular ions for these modified peptides.

DISCUSSION

Photoaffinity labeling using azidopurine analogues has been an effective technique for identifying nucleotide binding

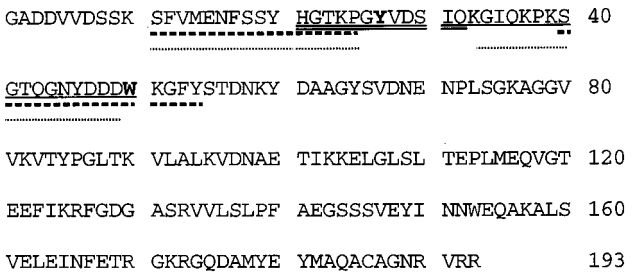

FIGURE 9: Sequence of diphtheria toxin fragment A (*8*). Peptides isolated after modification with [α-^{32}P]-8-N_3-NAD are designated under the amino acid sequence. Chymotryptic peptide 1 (H17−Q32) is denoted by double underline. Chymotryptic peptide 2 (K33−W50) is denoted by single underline. Lys-C peptide 1 (S11−P25) and peptide 2 (S40−Y54) are denoted with dashed lines. Arg-C peptide 1 (S11−P25) and peptide 2 (G34−D49) are denoted with dotted lines. Sites of modification are shown in boldface type. Tyr[27] is also a site of impeded chymotryptic cleavage, whereas Lys[51] is a site of impeded Lys-C cleavage.

domains in enzymes. 2-N_3-NAD (**2**) has been used as a photoprobe for the pyridine dinucleotide binding proteins lactate and glutamate dehydrogenase (*32*), *Clostridium botulinum* C3 ADP-ribosyl transferase (*31*), and 15-hydroxyprostaglandin dehydrogenase (*34*). More recently, it was used to label the NAD^+ binding site of the human poly(ADP-ribose) polymerase (PARP) catalytic domain (*35*). Where comparative data are available, photomodified residues are usually found within or adjacent to the binding site as defined by X-ray diffraction analysis. In this report, we used 8-N_3-NAD (**1**) as a photoaffinity label for diphtheria toxin fragment A (DT-A).

In any photoaffinity labeling study, experiments demonstrating the specificity of the photoinsertion reaction for the binding site are necessary. When [α-^{32}P]-8-N_3-NAD was incubated with DT-A, no photoincorporation was observed in the dark or when the photoprobe was irradiated immediately prior to addition of the enzyme. This indicates that the covalent modification occurred through a short-lived intermediate (i.e., a nitrene) formed directly from irradiation of the azido group. The specificity of photolabeling by **1** for the NAD^+ binding site was demonstrated by showing that photoincorporation saturates at low concentrations of **1** and that NAD^+ competes with **1** for a common binding site as evidenced by protection from photoderivatization in the presence of low concentrations of NAD^+. The K_d value (15 μM) for [α-^{32}P]-8-N_3-NAD obtained from saturation experiments (Figure 5A) was lower than the K_d value for NAD binding (35 μM) obtained from photoprotection experiments (Figure 5B). This implies tighter binding of [α-^{32}P]-8-N_3-NAD to the active site compared to that of NAD^+ and has been observed for several other NAD^+ binding proteins (*31*, *32*). The specificity of photoinsertion was further supported by comparing the effect of addition of NAD^+, ATP, AMP, adenosine, and adenine on photoincorporation. Maximum photoprotection was observed upon incubation with NAD followed by adenine, whereas ATP, AMP, and adenosine had little effect. The ability of the tested nucleotides and nucleosides to protect DT-A from photolabeling with **1** is consistent with the relative binding affinities of these compounds for DT-A as determined by Kandel et al. (*30*). Photoinsertion occurred with high efficiency especially after the reaction conditions were optimized. As the stoichiometry approached almost quantitative modification, a second ir-

radiation was not necessary. Cys^{186}, the only cysteine present in DT-A, was carboxymethylated and photolabeling of the carboxymethylated protein examined. Results indicate that an insignificant amount of labeling occurred through reaction with the cysteine SH.

It has been observed in previous studies that upon binding NAD^+ DT-A becomes resistant to trypsin digestion (*30*). The same effect was observed upon photoderivatization with 8-N_3-NAD. Despite its resistance to trypsin, derivatized DT-A could easily be proteolyzed by Lys C, Arg-C, or chymotrypsin. The electrophoretic mobility of the photolabeled peptides in SDS−PAGE appears to be considerably lower than that of the underivatized molecular mass markers based upon the expected size of the proteolytic peptides. This was confirmed as the sequences of the photoderivatized bands were determined. For example, the major modified peptide obtained from the chymotryptic digest His^{21}−Gln^{32} has a molecular mass of about 2 kDa, and the other peptide (Lys^{33}−Phe^{53}) has a molecular mass of about 3 kDa. A plot of log(MW) versus R_f predicted a molecular mass of about 7 kDa for the radiolabeled band which contained both the peptides. This anomalous mobility could be attributed to some disruption in the binding of SDS at the site of photoderivatization and has been observed in other instances (*36*, *37*).

When [α-^{32}P]-8-N_3-NAD was used to photolabel DT-A, two sites of modification were identified after purification and sequence analyses of the radiolabeled peptides. The primary sequence of DT-A and conclusions from these experiments are summarized in Figure 9. The two sites were recognized through repeated isolation of a set of overlapping peptide sequences from two separate regions in the protein, using three independent protease digestion strategies. The peptide His^{21}−Gln^{32} was isolated in three separate experiments from the chymotryptic digest of photolabeled DT-A, and in each case, the PTH derivative of Tyr^{27} predicted by the sequence in cycle 7 of the Edman degradation was undetectable. Several other tyrosyl residues were encountered in our sequencing, and in all other cases, the tyrosyl residue produced a PTH derivative in high yield. The second site of modification is best defined by Lys-C peptide 2 (Table 3), Ser^{40}−Lys^{59}, wherein Trp^{50} is the most probable site of modification. We have based our assignment on the abrupt decrease in the yield of PTH-Trp concomitant with cycle 11 and the lack of expected proteolytic cleavage by Lys-C at the adjacent susceptible lysyl residue (Lys^{51}). The assignment is slightly less convincing due to the position of this residue near the C-terminus of the isolated peptide and due to the possibility that tryptophan could have become chemically modified during peptide isolation and purification under acidic conditions. We also observe a lack of cleavage at Tyr^{46} in the overlapping chymotryptic peptide 2 (Lys^{33}−Phe^{53}). However, PTH-Tyr was detected in three experiments. This again supports Trp^{50} as a probable site of modification as lack of chymotryptic cleavage at Tyr^{46} could be attributed to the proximity of this residue to Trp^{50}.

Assignment of Tyr^{27} as the site of photoderivatization is fully in agreement with the crystallographic model of Bell and Eisenberg (Figure 10A) based upon dimeric diphtheria toxin bound to NAD^+ (*13*). This is also the first model in which the importance of Tyr^{27} was identified as a residue making hydrophobic contacts with the adenine ring. Our study with 8-N_3-NAD also places Tyr^{27} close to the adenine ring.

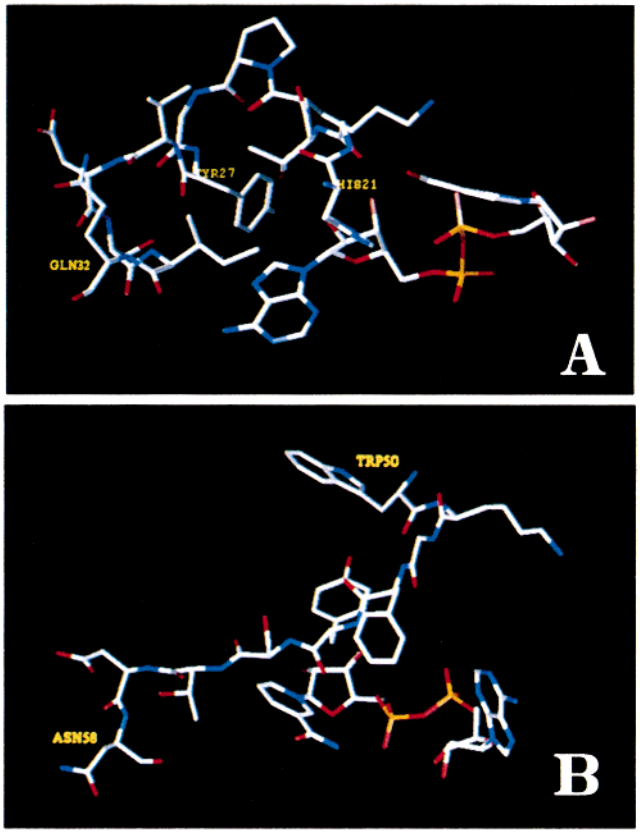

FIGURE 10: NAD^+ binding in the vicinity of the photoderivatized peptides. Panel A shows NAD and H21−Q32. The purine ring of NAD is close to the aromatic ring of Y27. Panel B shows NAD and W50−N58. The purine of the dinucleotide is both oriented incorrectly and distant from the indole ring of W50. Coordinates for the bound dinucleotide and the designated amino acids were taken from the structure of diphtheria toxin bound to NAD as deposited in the Protein Data Bank (1TOX).

Trp^{50} is a conserved residue in ADP-ribosylating toxins such as DT, *Pseudomonas areuginosa* exotoxin A (ETA), pertussis toxin (PT), and cholera toxin (CT). The importance of Trp^{50} to NAD^+ binding has been suggested by site-directed mutagenesis studies. Results from mutation of Trp^{50} to alanine and phenylalanine indicated that Trp^{50} was a major determinant of NAD^+ affinity (*38*). Our assignment of Trp^{50} as the other photoinsertion site is more difficult to rationalize with Bell and Eisenberg's crystallographic model based upon DT, because this model predicts that Trp^{50} is about 10 Å from the nearest point in the adenine ring, a distance which would seem to be too far for facile photomodification (Figure 10B). However, it is known that fragment A undergoes a structural transition upon NAD^+ binding (*12*), and it is possible that movement of two structural loops in DT-A brings Trp^{50} near the adenine ring in the DT-A−NAD^+ complex. Another possibility for explaining covalent modification of Trp^{50} is that an alternate binding mode is available to NAD^+ and 8-N_3-NAD^+. The incompatibility with the crystallographic model could also be attributed to the difference under experimental conditions between the solid phase study and our solution phase study conducted at pH 6, or to differences between the structure of NAD^+ bound to DT and NAD^+ bound to DT-A.

On the basis of our result, we conclude that when [α-^{32}P]-8-N_3-NAD is used to photolabel DT-A, Tyr^{27} is the major site of modification and constitutes approximately 70% of the total photoderivatization reaction. A second probable site of modification appears to be Trp^{50}.

ACKNOWLEDGMENT

We thank Prof. Barbara Carter (Department of Chemistry, University of Toledo) and Dr. Sushma Ramsinghani (Department of Medicinal and Biological Chemistry, University of Toledo) for assistance in the production of the radiolabeled photoprobes.

REFERENCES

1. Collier, R. J. (1975) *Bacteriol. Rev. 39*, 54−85.
2. Pappenheimer, A. M., Jr. (1977) *Annu. Rev. Biochem. 46*, 69−94.
3. Wilson, B. A., and Collier, R. J. (1992) *Curr. Top. Microbiol. Immunol. 175*, 27−41.
4. DeLange, R. J., Drazin, R. E., and Collier, R. J. (1976) *Proc. Natl. Acad. Sci. U.S.A. 73*, 69−72.
5. DeLange, R. J., Williams, L. C., and Collier, R. J. (1979) *J. Biol. Chem. 254*, 5827−31.
6. DeLange, R. J., Williams, L. C., Drazin, R. E., and Collier, R. J. (1979) *J. Biol. Chem. 254*, 5838−42.
7. Drazin, R. E., Collier, R. J., Williams, L. C., and DeLange, R. J. (1979) *J. Biol. Chem. 254*, 5832−7.
8. Greenfield, L., Bjorn, M. J., Horn, G., Fong, D., Buck, G. A., Collier, R. J., and Kaplan, D. A. (1983) *Proc. Natl. Acad. Sci. U.S.A. 80*, 6853−7.
9. Ratti, G., Rappuoli, R., and Giannini, G. (1983) *Nucleic Acids Res. 11*, 6589−95.
10. Bennett, M. J., Choe, S., and Eisenberg, D. (1994) *Protein Sci. 3*, 1444−63.
11. Bennett, M. J., and Eisenberg, D. (1994) *Protein Sci. 3*, 1464−75.
12. Weiss, M. S., Blanke, S. R., Collier, R. J., and Eisenberg, D. (1995) *Biochemistry 34*, 773−81.
13. Bell, C. E., and Eisenberg, D. (1996) *Biochemistry 35*, 1137−49.
14. Bell, C. E., and Eisenberg, D. (1997) *Biochemistry 36*, 481−8.
15. Carroll, S. F., and Collier, R. J. (1984) *Proc. Natl. Acad. Sci. U.S.A. 81*, 3307−11.
16. Carroll, S. F., and Collier, R. J. (1994) *Methods Enzymol. 235*, 631−9.
17. Papini, E., Santucci, A., Schiavo, G., Domenighini, M., Neri, P., Rappuoli, R., and Montecucco, C. (1991) *J. Biol. Chem. 266*, 2494−8.
18. Carroll, S. F., Barbieri, J. T., and Collier, R. J. (1988) *Methods Enzymol. 165*, 68−76.
19. Carroll, S. F., and Collier, R. J. (1988) *Mol. Microbiol. 2*, 293−6.
20. Carroll, S. F., and Collier, R. J. (1988) *Methods Enzymol. 165*, 218−25.
21. Chung, D. W., and Collier, R. J. (1977) *Biochim. Biophys. Acta 483*, 248−57.
22. Koberstein, R. (1976) *Eur. J. Biochem. 67*, 223−9.
23. Czarnecki, J., Geahlen, R., and Haley, B. (1979) *Methods Enzymol. 56*, 642−53.
24. Hughes, N. A., Kenner, G. W., and Todd, A. (1957) *J. Chem. Soc.*, 3733−8.
25. Michelson, A. M. (1964) *Biochim. Biophys. Acta 91*, 1−13.
26. Kim, H., and Haley, B. E. (1990) *J. Biol. Chem. 265*, 3636−41.
27. Ames, B. (1966) *Methods Enzymol. 8*, 115−8.
28. Lodaya, R., and Slama, J. T. (1999) *J. Labelled Compd. Radiopharm.* (in press).
29. Schagger, H., and von Jagow, G. (1987) *Anal. Biochem. 166*, 368−79.
30. Kandel, J., Collier, R. J., and Chung, D. W. (1974) *J. Biol. Chem. 249*, 2088−97.
31. Chavan, A. J., Nemoto, Y., Narumiya, S., Kozaki, S., and Haley, B. E. (1992) *J. Biol. Chem. 267*, 14866−70.
32. Kim, H., and Haley, B. (1991) *Bioconjugate Chem. 2*, 142−7.
33. King, S. M., Kim, H., and Haley, B. E. (1991) *Methods Enzymol. 196*, 449−66.
34. Chavan, A. J., Ensor, C. M., Wu, P., Haley, B. E., and Tai, H. H. (1993) *J. Biol. Chem. 268*, 16437−42.
35. Kim, H., Jacobson, M. K., Rolli, V., Menissier-de Murcia, J., Reinbolt, J., Simonin, F., Ruf, A., Schulz, G., and de Murcia, G. (1997) *Biochem. J. 322*, 469−75.
36. Salvucci, M. E., Chavan, A. J., and Haley, B. E. (1992) *Biochemistry 31*, 4479−87.
37. Mimura, C. S., Admon, A., Hurt, K. A., and Ames, G. F. (1990) *J. Biol. Chem. 265*, 19535−42.
38. Wilson, B. A., Blanke, S. R., Reich, K. A., and Collier, R. J. (1994) *J. Biol. Chem. 269*, 23296−301.

BI991528N